Chemistry & Biology, Vol. 11, 1081–1091, August, 2004, ©2004 Elsevier Ltd. All rights reserved. DOI 10.1016/j.chembiol.2004.05.019

Design and Validation of a Bifunctional Ligand Display System for Receptor Targeting

Limor Chen, Amado J. Zurita, Peter U. Ardelt, Ricardo J. Giordano, Wadih Arap, and Renata Pasqualini*
The University of Texas
M.D. Anderson Cancer Center
1515 Holcombe Boulevard
Houston, Texas 77030

Summary

Here we developed a bacteriophage display particle designed to serve as a bifunctional entity that can target tumors while delivering an agent. We engineered a chimera phage vector containing a pIII-displayed α_v integrins-targeting moiety and a pVIII-displayed streptavidin binding adaptor moiety. By using the chimeric phage particle, targeting of α_v integrins on cells in culture and tumor-related blood vessels was shown through different applications, including luminescent quantum dots localization, surface plasmon resonance-based binding detection, and an in vivo tumor model. The strategy validated here will accelerate the discovery and characterization of receptor-ligand binding events in high throughput, and cell-specific delivery of diagnostics or therapeutics to organs of choice without the need for chemical conjugation.

Introduction

Bispecific compounds can be designed for targeted delivery to cell surface receptors associated with disease; however, chemical conjugation or coupling of adaptor proteins often results in loss of receptor-ligand binding capability or insoluble products [1]. On the other hand, filamentous bacteriophage are versatile display systems, and genetic manipulation renders them suitable biological reagents [2–7]. A commonly used phage display vector is the filamentous bacteriophage M-13 and its derivative fd-tet [8]. Display of peptides and proteins has been achieved in five structural capsid proteins (pIII, pVI, pVII, pVIII, and pIX), but many studies use fusions with the phage pIII (minor capsid protein) or the pVIII (major capsid protein) because they are efficient presentation systems [2, 9].

Despite extensive knowledge of the bacteriophage life cycle and biology [2] and existing data to show that the simultaneous display of ligands on different proteins can generate a bifunctional phage, such constructs have been restricted to in vitro applications such as enzyme-linked immunosorbent assay (ELISA). For example, Light and Lerner have created so called "PhoPhabs" by incorporating alkaline phosphatase and antibody (Ab) Fab's from combinatorial libraries on a filamentous phage [10], and Bonnycastle et al. have generated a bifunctional phage as a strategy to capture phage on fibrinogen or streptavidin [11] to perform ELISA.

Here we expand this concept by constructing and validating a bifunctional phage that displays an integrin binding motif and a streptavidin binding motif. We also show six potential applications for this dual-display particle both in vitro and in vivo.

Results

Design of the Chimeric Phage Vector

We chose two well-characterized phage clones, RGD-4C and R5C2, to construct a bifunctional display model system. RGD-4C phage displays on pIII the double-cyclic CDCRGDCFC peptide that targets α_v integrins. This peptide contains an embedded Arg-Gly-Asp (RGD) motif found in several extracellular matrix proteins [12] and allows targeting of tumor-related angiogenic blood vessels [13]. R5C2 phage display the cyclic ANRLCHPQFPCTSHE peptide—isolated by panning an f88-Cys5 phage display library on immobilized streptavidin—on approximately 150–300 of the 3900 copies of pVIII (NCBI accession #AF246454). The R5C2 peptide (among other "biotin-like" peptides) contains the streptavidin binding sequence His-Pro-Gln (HPQ), which conveniently binds streptavidin at a lower affinity than biotin ($K_d \sim 2–5 \times 10^{-8}$ and 4×10^{-14}, respectively) [14, 15]. In view of these features, we hypothesized that incorporating HPQ onto the pVIII coat of a chimera phage targeted to a cell surface receptor would enable (1) reversible coupling of streptavidin-coupled bioconjugates or (2) immobilization on streptavidin-coated surfaces, beads, or luminescent quantum dots (Qdots). These functional properties would be incorporated on a single phage particle while preserving the targeting of α_v integrin-expressing cells mediated by the pIII-displayed RGD-4C peptide.

To produce the chimeric phage, we used the vectors fUSE5 and f88, which share a similar genomic backbone [2, 5, 8]. We extracted genomic *cis*-acting elements from each plasmid and reassembled them to create a chimera phage. DNA isolated from RGD-4C (a fUSE5 derivative) and R5C2 (a f88 derivative) phage clones were digested, and fragments with the corresponding cassettes were ligated to create an RGD-4C/R5C2 phage construct (hereafter termed chimera phage) in which pIII and pVIII are mapped to their locations (Figure 1A). The resulting coat is a mosaic displaying wild-type and recombinant pVIII proteins (Figure 1B).

Testing the Streptavidin Binding Capacity of the Chimera Phage

To test the streptavidin binding properties of the chimera, we quantified phage binding to streptavidin-coated plates by ELISA using an anti-phage Ab. The chimera phage bound to immobilized streptavidin at levels similar to those of the parental R5C2 phage. Insertless phage (fd-tet) and parental RGD-4C phage did

*Correspondence: rpasqual@mdanderson.org

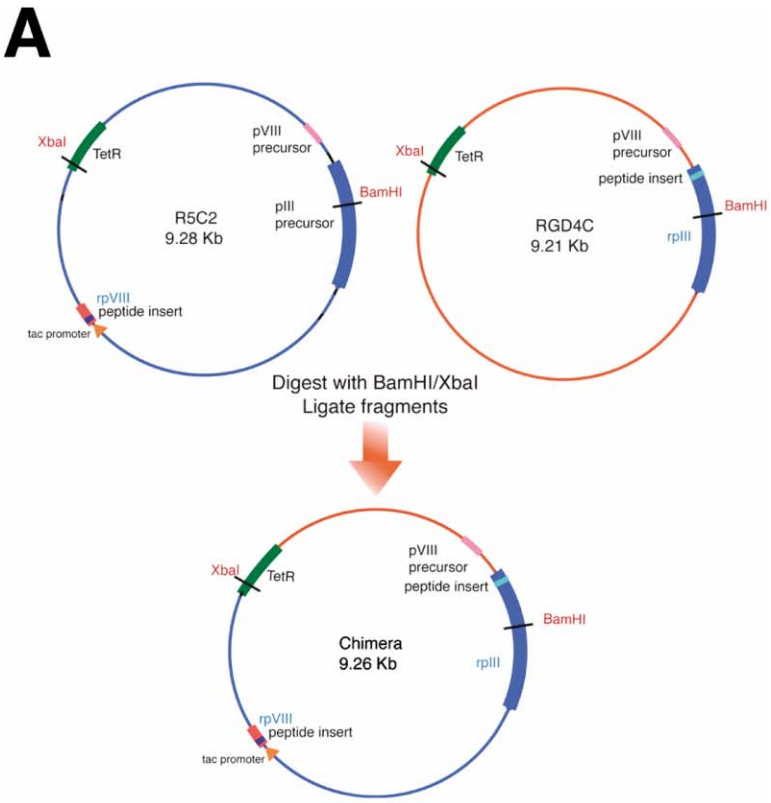

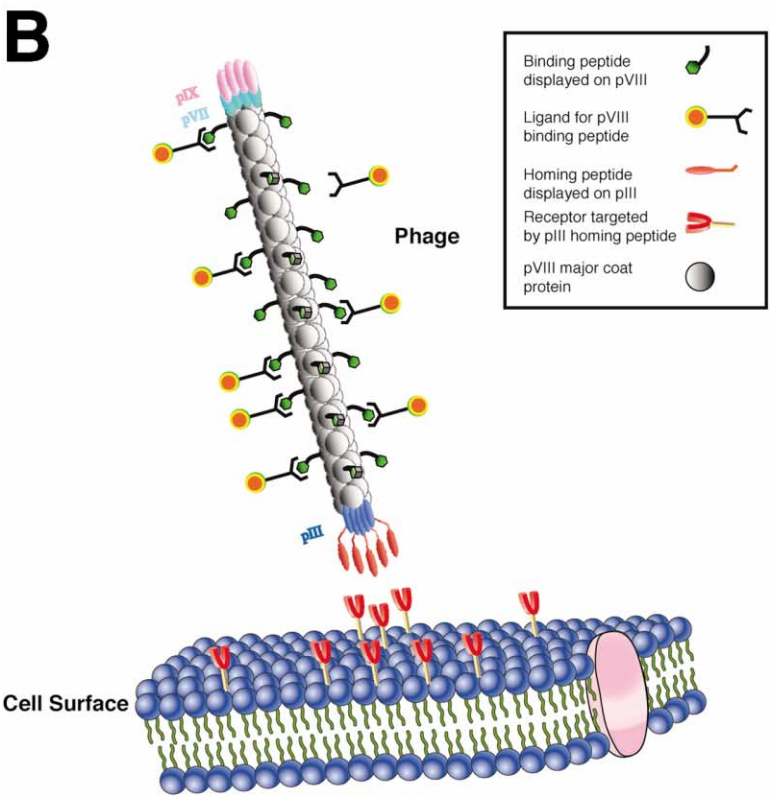

Figure 1. Bifunctional Chimera Phage Vector Design and Construction

(A) Scheme of the construction of chimera phage with homing and adaptor motifs. Replicative forms of the streptavidin binding phage R5C2, derived from type f88-Cys5 pVIII display vector, and the α_v integrin binding phage RGD-4C, derived from a fUSE5 pIII display vector, were digested with BamHI and XbaI. Swapping of functional fragments from each vector created a chimera phage vector containing pVIII (red) and pIII (blue) fusion peptide display domains. *Tac* promoter drives transcription from the recombinant pVIII cassette (orange triangle). pVIII: major coat protein VIII; pIII: minor coat protein III; rpVIII: recombinant pVIII; rpIII: recombinant pIII; TetR: tetracycline resistance element.

(B) Chimera phage particle representation. The chimera phage displays the targeting peptides on the pIII minor coat protein and an adaptor on the pVIII major coat protein.

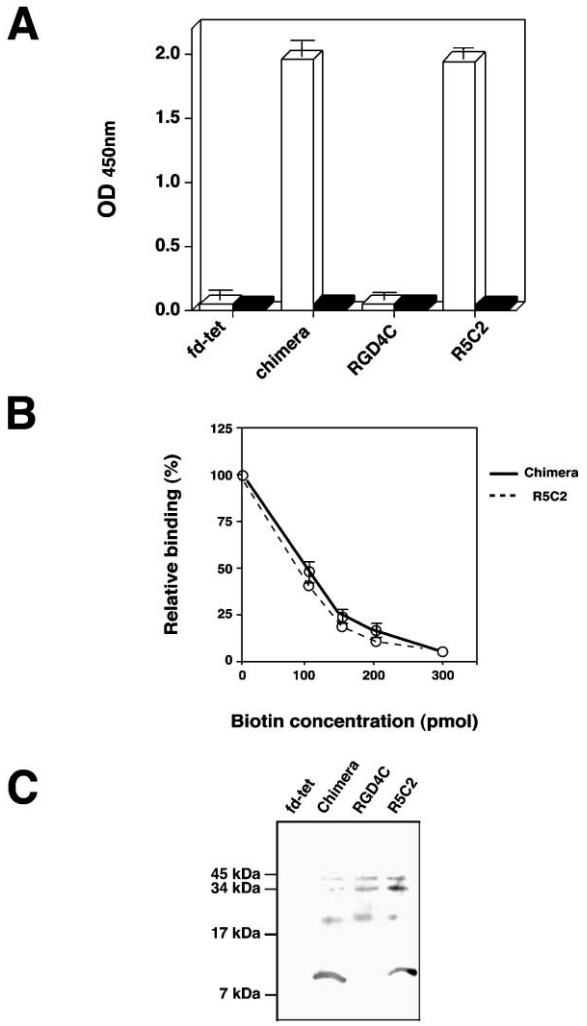

Figure 2. Chimera Phage Binding to Streptavidin

(A) Binding of the chimera phage to streptavidin-coated plates by ELISA. Phage were incubated with streptavidin (white columns) or BSA (black columns). An anti-pVIII monoclonal antibody-HRP conjugate was used for detection. Results are mean ± SEM of triplicate wells from two independent experiments.

(B) Biotin inhibition of phage binding. Biotin was incubated with each phage before the admixture was added to the coated wells. Results are expressed as percent binding of phage alone (set to 100%). Shown are the mean ± SEM from triplicate wells. Inhibitions of R5C2 phage (dashed line) and chimera phage (solid line) were similar.

(C) Streptavidin blot hybridization of phage resolved by SDS-PAGE. Membranes with the transferred proteins were reacted with HRP-streptavidin and processed. Unique ~8 kDa bands are visible only in the phage displaying streptavidin binding motifs.

not show binding above the background level, and none of the phage clones bound to BSA (Figure 2A). Next, we showed that biotin inhibits the binding of the chimera and the R5C2 phage to streptavidin in a similar, dose-dependent manner (Figure 2B). The level of binding of RGD-4C and fd-tet phage was very low and was not affected by biotin (data not shown). Together, these results demonstrate the specificity of the chimera phage toward streptavidin. We used Western blot analysis to show that binding to streptavidin is mediated by recombinant pVIII fusion protein containing the HPQ motif. Unique ~8 kDa bands were observed for the chimera phage and positive control (R5C2 phage), reflecting the mobility of recombinant pVIII. We found no reactivity for the control fd-tet and RGD-4C clones (Figure 2C) or binding for any of the phage clones in the presence of biotin. Additional reactive bands in this blot represent nonspecific binding of streptavidin to other phage proteins and/or to contaminating species from the host bacteria. These data show that the recombinant pVIII proteins displaying HPQ motifs on the chimera phage retain their streptavidin binding capacity.

Cell-Surface Integrin Binding Characteristics of the Chimera Phage

We next evaluated the binding of the RGD-4C motifs displayed on pIII of the chimera to cells expressing $\alpha_v\beta_3$ and $\alpha_v\beta_5$ integrins to establish specificity. pIII is composed of three domains separated by glycine-rich regions. We produced recombinant fusion proteins of domain 1 displaying an RGD-4C peptide ($pIII_{D1}$-RGD-4C) or no peptide ($pIII_{D1}$-fd) for competition assays. In the fUSE5-based vector, pIII displays peptides at the amino terminus of D1 ($pIII_{D1}$; Figure 3A) [2, 5]. The $pIII_{D1}$ presentation system was designed to display peptides in a "phage-like" context, with the advantage of a substantially lower cost than synthetic peptides. Pilot studies (data not shown) demonstrated that the $pIII_{D1}$-presented recombinant peptides used here were as active as the corresponding synthetic peptides at equimolar peptide concentrations.

We showed that $pIII_{D1}$-RGD-4C recombinant protein promoted adhesion of KS1767 cells (Figure 3B), which express α_v integrins in high levels and resemble the phenotype of activated endothelial cells [16], whereas $pIII_{D1}$-fd did not (Figure 3C). Cell attachment was inhibited by the synthetic peptide RGD-4C but not by the negative control peptide CRGESP (data not shown). These data confirm that cell adhesion in this system is specific and RGD dependent. Having shown that the recombinant fusion RGD-4C is functional outside of the phage context, we tested the capacity of the chimera phage to specifically bind to α_v integrins expressed in the cell surface. Phage were incubated with KS1767 cells, with or without recombinant fusion proteins. Cell-bound phage were then separated from unbound phage by an aqueous-organic phase separation method [16]. Chimera and parental RGD-4C phage specifically bound to cells at levels up to 45-fold of that in the parental R5C2 clone, which does not bind to α_v integrins. Mixing $pIII_{D1}$-fd fusion protein with phage before incubation with cells had no effect on phage binding. However, use of $pIII_{D1}$-RGD-4C protein resulted in a marked reduction in binding for the chimera and RGD-4C phage; $pIII_{D1}$-fd had no effect on the control R5C2 phage (Figure 3D). We also tested binding of the chimera to KS1767 cells by direct immunostaining of cell-bound phage. Phage were added to cell monolayers and detected by staining with an anti-phage Ab (Figures 3E–3L). Chimera phage (Figure 3E) bound to cells in a manner similar to parental RGD-4C phage (Figure 3F). The $pIII_{D1}$-RGD-4C fusion

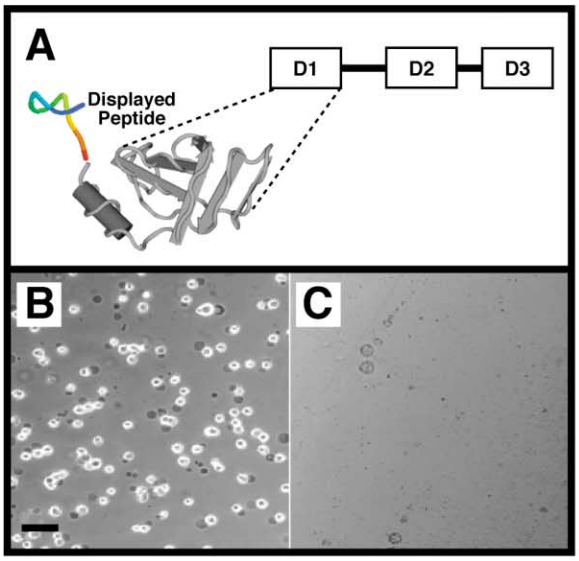
A
D1
D2
D3
Displayed
Peptide
B
C

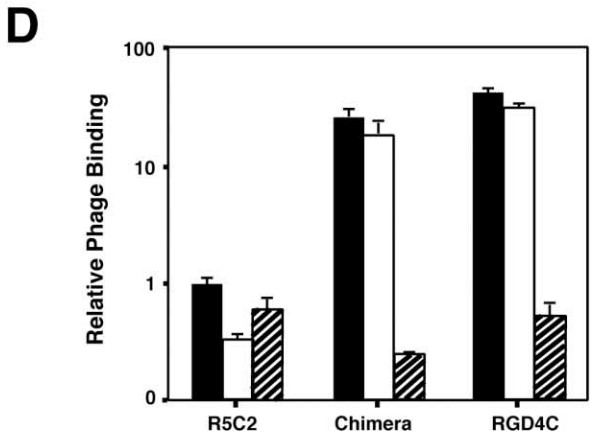
D
Relative Phage Binding
100
10
1
0
R5C2
Chimera
RGD4C

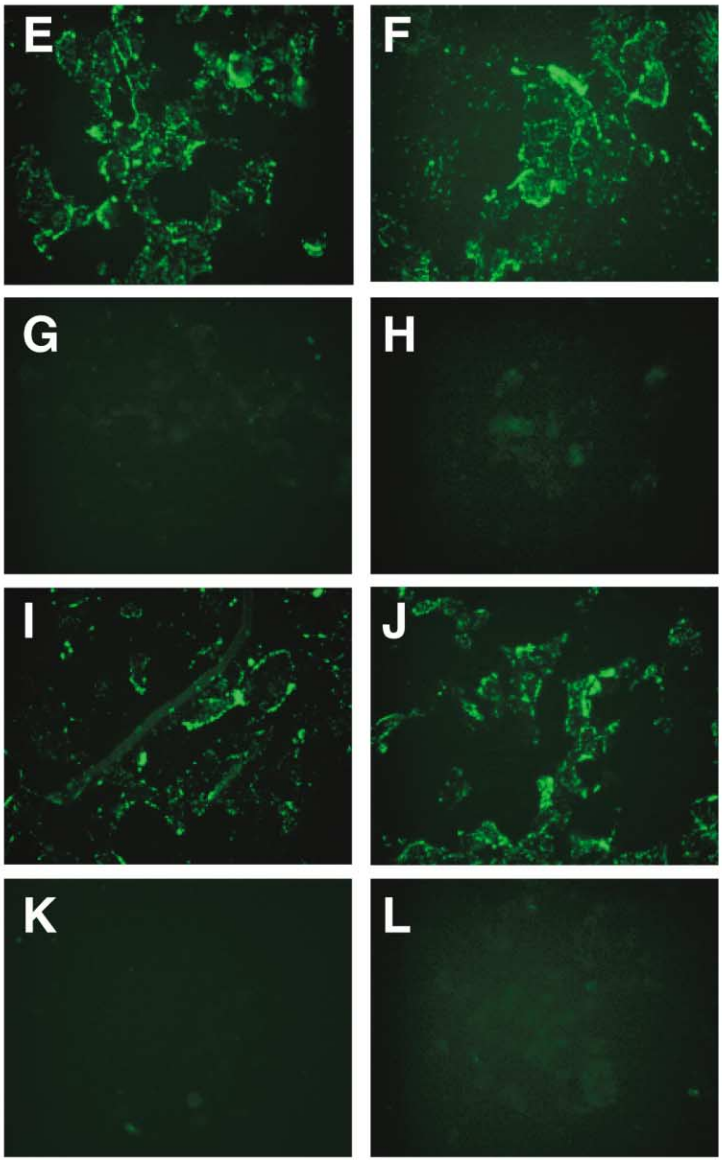
E
F
G
H
I
J
K
L

protein inhibited binding of these clones (Figures 3G and 3H), whereas $pIII_{D1}$-fd had no effect (Figures 3I and 3J). Insertless fd-tet phage (Figure 3K) and parental R5C2 phage (Figure 3L) were not detected when tested under identical conditions. These data show that binding of the chimera to α_v integrin-expressing cells is mediated by the RGD-4C motif and is not affected by the introduction of multiple HPQ motifs on pVIII coat proteins.

Applications of the Bifunctional Phage In Vitro

Several different in vitro applications were devised. First, we used a cell-overlay assay in which phage were immobilized on a streptavidin-coated plate and subsequently α_v integrin-expressing cells were added. In wells coated with control phage, only 4%–7% of the added cells adhered to the well surface, whereas in wells coated with the chimera, over 75% of the input was recovered (Figure 4A).

Second, we performed a binding assay in which phage were incubated with streptavidin-coated magnetic beads in suspension and magnetically separated. We then added α_v integrin-expressing cells to the phage-coated beads. After additional magnetic separation, cells were plated and monitored after an overnight incubation at 37°C. The number of attached cells in wells from the chimera-reacted streptavidin beads was much larger than the number from negative controls including fd-tet phage, RGD-4C phage, or beads alone (Figure 4B); R5C2 phage did not promote cell adhesion despite efficient binding to beads.

Third, we visualized phage binding to α_v integrin-expressing cell monolayers by using fluorescent dye-containing microspheres coated with streptavidin as a phage detection tool. These microspheres are 40 nm in diameter and fluoresce within the orange-red emission spectrum [17]; such features facilitate imaging applications because histologic sections generally autofluoresce within the green spectrum. Chimera or control phage were added to cell monolayers and allowed to bind, followed by addition of streptavidin-coated or fluorescent microspheres without coating (Figures 4C–4H). In the wells to which the chimera phage were added, streptavidin beads were detected in high numbers (Figure 4C). In contrast, we found low levels of binding with control beads (Figure 4D). Moreover, RGD-4C phage (Figure 4E) or fd-tet phage (Figure 4G), which do not bind streptavidin, showed only background fluorescence. To show that the beads were reactive to streptavidin, RGD-4C phage were added to the cell monolayer and reacted with an anti-phage and a biotinylated secondary Ab. Streptavidin-coated beads were then added, and marked fluorescence was observed (Figure 4F), validating the reactivity of RGD-4C phage with cells and the biotin binding activity of the microspheres. R5C2 phage do not bind to the cells; therefore, no significant fluorescence was detected (Figure 4H). Cells incubated with RGD-4C phage and uncoated beads showed only background fluorescence (data not shown).

Fourth, we evaluated the chimera phage in a biosensor (BIAcore) that monitors molecular interactions by using surface plasmon resonance [18]. The streptavidin binding moiety on the phage surface was used to immobilize a large number of particles on the surface of a streptavidin-coated sensor chip, and α_v integrin-expressing cells were then injected over the phage-coated surface to detect real-time binding. The sensor chip was layered with chimera or R5C2 phage, and surface plasmon resonance signals were measured (Figure 4I). The chimera phage-coated channel showed a higher response to the cells than did the R5C2 phage-coated channel, whereas the control channel coated with streptavidin alone showed only background cell binding levels (data not shown). The on-rate of cell mass buildup on the chip surface for the chimera phage was over 170% that of control R5C2 phage, as calculated from the slope of the log phase in the sensograms. In spite of some variation related to the ligand (phage) and analyte (cells), the relative effect observed in the experiments (binding versus no binding) was consistent.

Fifth, we targeted a fluorescently labeled phage to the cell surface by using nanometer-scale Qdots; the emission spectrum of the crystals has superior optical properties because it is very narrow and almost independent of the excitation wavelength, whereas the fluorescence is bright and photostable [19, 20]. We created a fluorescently labeled phage by mixing chimera or control phage with the streptavidin-coated Qdots. The complex was incubated with adherent KS1767 cells for 2 (Figures 5A, 5C, and 5E) or 24 hr (Figures 5B, 5D, and 5F). We monitored the cells for phage binding and internalization by staining with an anti-phage and a fluorescein isothiocyanate (FITC)-conjugated secondary Ab. Cell-bound RGD-4C phage could only be detected when an anti-phage Ab was used (Figure 5A), whereas the

Figure 3. Validation of Binding of Chimera Phage to Cells Expressing α_v Integrins

(A) pIII domain 1 ($pIII_{D1}$) fusion peptide used in binding inhibition studies. A detailed view of the putative structure of the entire pIII protein including the domain 1 recombinant protein designed in this study is represented.

(B and C) Adhesion of cells expressing $\alpha_v\beta_3$ and $\alpha_v\beta_5$ integrins (KS1767) to plates coated with the recombinant fusion proteins displayed on pIII of the chimera phage ($pIII_{D1}$-RGD-4C) (B) or the domain 1 construct of the fd-tet fusion protein ($pIII_{D1}$-fd) (C). KS1767 cells were added and allowed to adhere, and the wells were rinsed. Shown are phase-contrast images of representative wells from each group. Scale bar, 10 μm.

(D) Binding inhibition of streptavidin binding phage R5C2, α_v integrin binding phage RGD-4C, and bifunctional chimera phage to KS1767 cells. Phage were reacted with KS1767 cells, separated, and recovered from the mixture by an aqueous-organic phase separation. Inhibitions were performed with recombinant pIII fusion proteins. Binding of phage only (filled columns), phage plus $pIII_{D1}$-RGD-4C (hatched columns), and phage plus $pIII_{D1}$-fd (empty columns) is shown. Results are expressed as the mean binding of phage to cells relative to R5C2 phage (set to 1) ± SEM.

(E–L) Immunofluorescence of phage binding to KS1767 cells. Cell monolayers were overlaid with the chimera (E, G, and I), RGD-4C phage (F, H, and J), fd-tet phage (K), or R5C2 parental clone (L). To test inhibition, $pIII_{D1}$-RGD-4C (G and H) or $pIII_{D1}$-fd (I and J) proteins were added. Phage were detected with a FITC-labeled anti-phage antibody. Representative results from three independent experiments are shown. Scale bar, 10 μm.

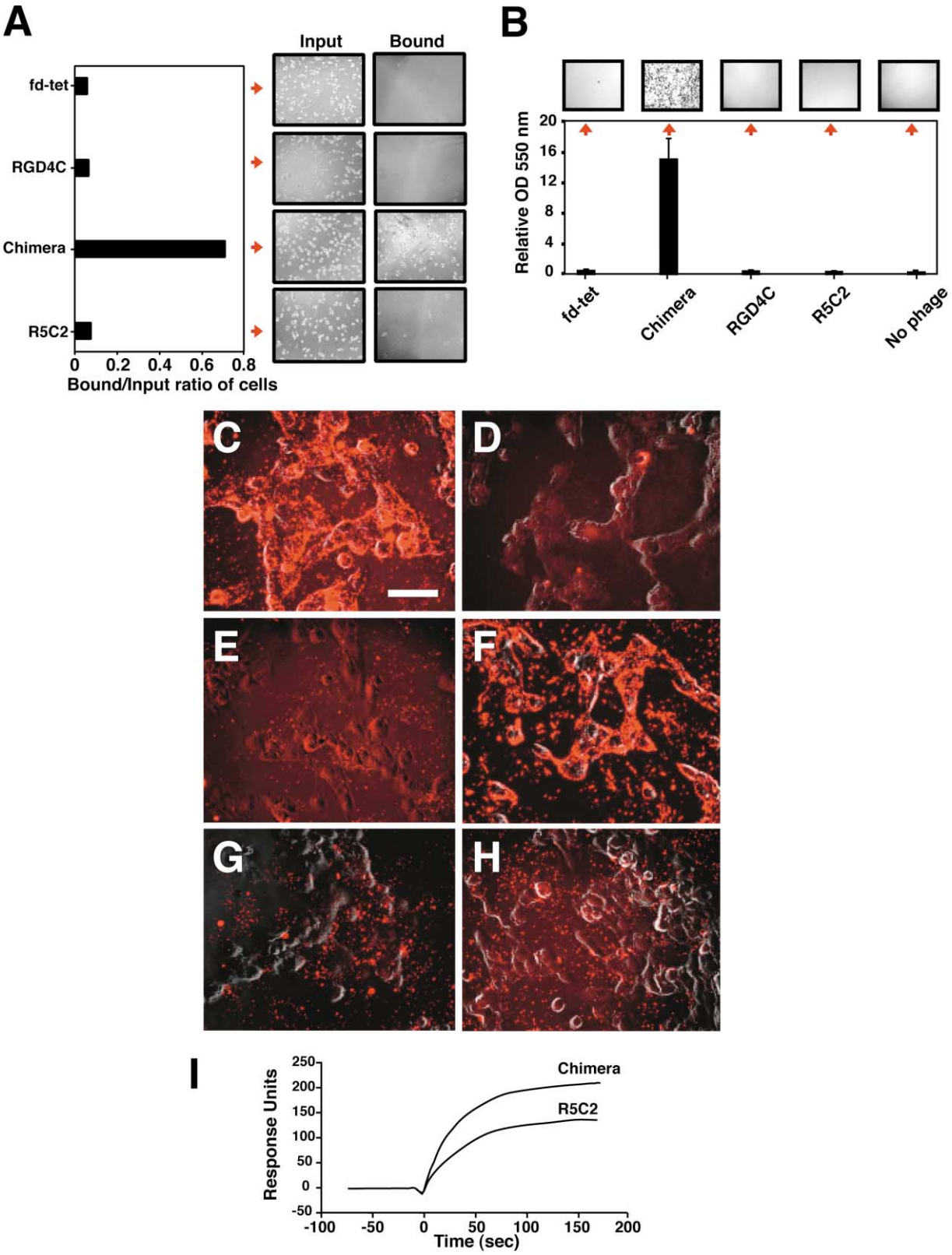

Figure 4. Binding of the Chimera Phage through Both Displayed Motifs

(A) Cell overlay assay for phage binding to KS1767 cells and streptavidin. Phage were incubated in streptavidin-coated plates, followed by the addition of cells. After incubation, adherent cells were counted. The relative fraction of cells remaining on the well surface after washings is presented as a bound/input ratio (left panel), and representative images from each condition are shown (right panels). Assays were performed in triplicates, with similar results.

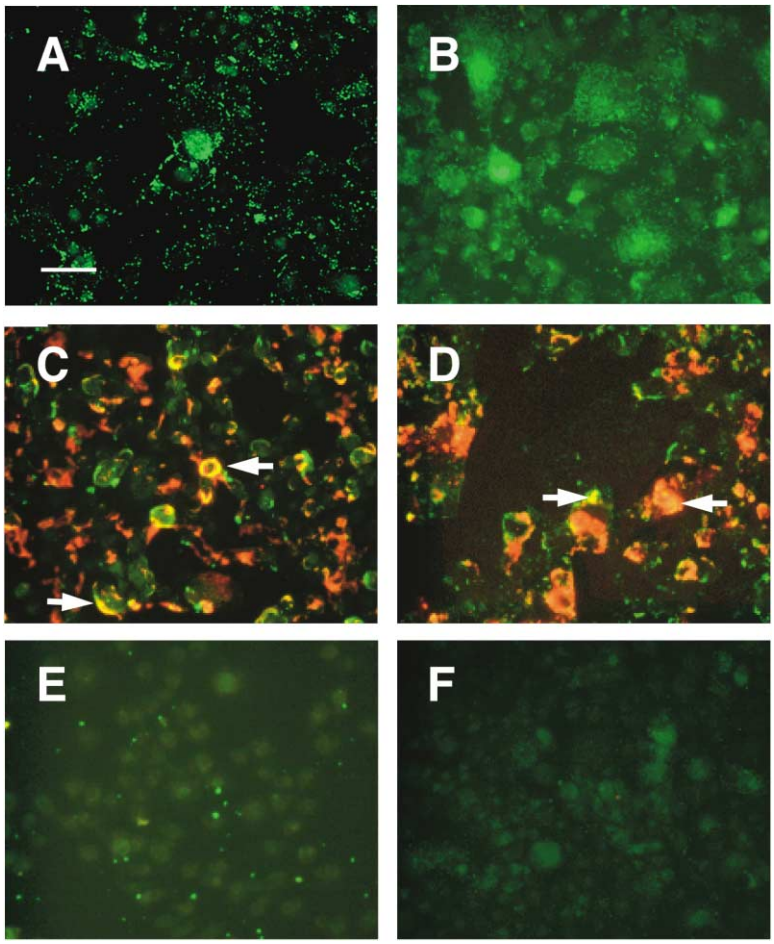

Figure 5. Targeting Qdots-Streptavidin to Cells

RGD-4C phage (A and B), chimera phage (C and D), or R5C2 phage (E and F) were reacted with Qdot 605 streptavidin, and the comixture was then added to adherent KS1767 cells and incubated for 2 hr (A, C, and E) or 24 hr (B, D, and F). Cells incubated for 2 hr with phage were then stained with anti-phage antibody and a secondary FITC conjugate and fixed. Cells incubated for 24 hr with the phage were stripped of any cell membrane-bound phage particles and then permeabilized and stained with anti-phage antibody in a similar manner and fixed. Each treatment was repeated twice. Shown are representative images acquired with an epi-fluorescent microscope by using the UV-blue excitation filter. White arrows point to cells showing colocalized yellow fluorescence. Scale bar, 10 μm.

R5C2 clone showed background fluorescence (Figure 5E). As expected, the chimera phage displayed dual staining with both red and green fluorescence (colocalization evident by yellow; Figure 5C). Cells incubated for 24 hr with RGD-4C or chimera phage internalized the phage, as shown by green (RGD-4C; Figure 5B) and yellow (chimera phage; Figure 5D). In contrast, cells incubated with the R5C2 clone displayed only background fluorescence (Figure 5F). Heterogeneity of staining in Figures 5C and 5D may reflect variations in the chimera phage binding of Qdots and partial masking of the FITC green fluorescence by the stronger red signal of the Qdots. These results establish the capacity of a phage-Qdot complex to specifically recognize and target cell surface receptors and to be internalized as a complex into the cytoplasm.

Tumor Targeting with Chimera Phage In Vivo

Having shown the viability of using the bifunctional construct in vitro, we set out to develop a targeting application in vivo as proof-of-principle for the chimera phage. We adopted a well-established mouse mammary gland tumor model [21] to show the efficiency of the bifunctional phage in targeting tumors in vivo. EF43.*fgf-4* cells, which are retrovirally infected with the *fgf*-4 gene, consistently form highly vascularized tumors in immunocompetent mice [21].

Mice bearing tumors with 8–10 mm in diameter re-

(B) KS1767 cell capturing by chimera phage. Phage were mixed with streptavidin-coated magnetic beads and allowed to react. After magnetic separation, cells were mixed with the beads, separated, plated, and quantified by crystal violet staining. Shown are the absorbances after dye solubilization (lower panel) and phase contrast micrographs of representative wells from each phage group (upper panels).

(C–H) Cell-surface labeling with chimera or control phage. KS1767 cell monolayers were incubated with chimera (C and D), RGD-4C (E and F), fd-tet (G), or R5C2 phage (H). Subsequently, streptavidin-coated fluorescent beads (C, E, G, and H) or control beads (D) were added and allowed to react with the phage. For the anti-M13 pVIII antibody cells, incubation with a secondary biotinylated antibody was followed by the addition of streptavidin-coated microspheres (F). The plate was observed under a fluorescence microscope. Images were acquired by simultaneously using a red fluorescence filter and a bright light field. Representative images from three independent experiments with duplicate wells for each test group, with similar results, are shown. Scale bar, 10 μm.

(I) Interaction of the chimera phage with KS1767 cells by BIAcore. After 10^{11} TU/ml of chimera or R5C2 phage were coated onto streptavidin BIAcore chips at similar levels, chips were subjected to a KS1767 single-cell suspension flow (at 10^5 cells/ml). Responses were recorded to saturation. Shown are representative sensograms acquired from the two phage-coated channels normalized to the injection point (time zero).

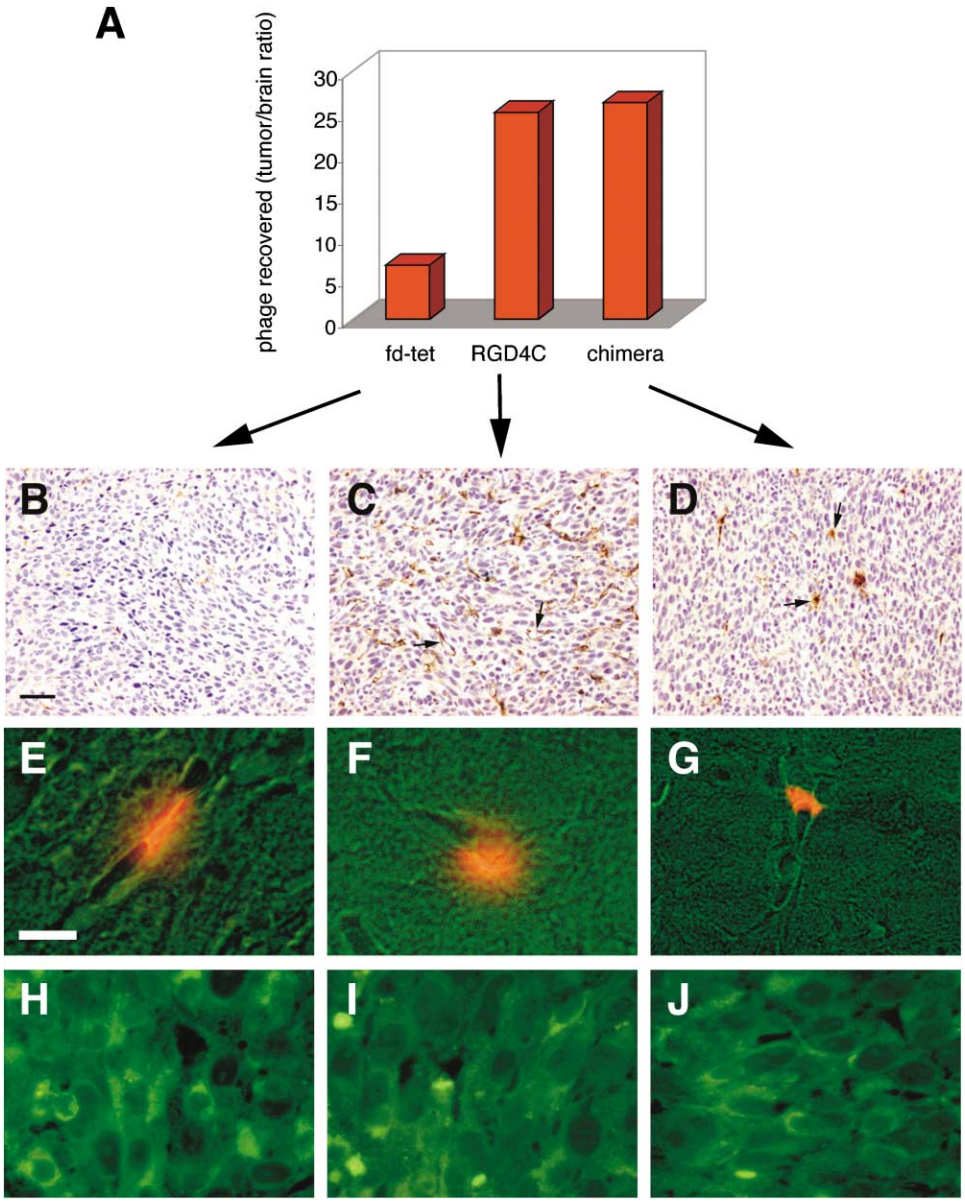

Figure 6. In Vivo Targeting of Chimera-Qdot Complex to Tumors

(A) Phage recovered from tissues of mice that received phage/Qdot complexes intravenously. Tumor/control organ homing ratios for different phage clones are presented.

(B–D) Immunostaining for phage in mice injected with phage/Qdot complexes. Anti-phage antibody reveals strong staining of blood vessels in the RGD-4C/Qdot-injected mouse (black arrows in [C]) and a larger aggregated pattern for the chimera-Qdot-injected mouse (black arrows in [D]). Scale bar, 20 μm.

(E–J) Fluorescent microscopy of tissues injected with phage/Qdot complexes. Large fluorescent aggregates are present in a tumor from a mouse injected with the chimera-Qdot complex (E–G), but no signal is present in tumors from RGD-4C/Qdot complex-injected mouse (H–J). Scale bar, 10 μm.

ceived phage clones reacted with Qdots streptavidin intravenously. After perfusion, tumor and control organs were surgically removed. Brain was chosen as a standard reference organ because of its low phage tissue uptake [13, 22]. We found preferential homing of the RGD-4C and the chimera phage to the tumor (Figure 6A). Specifically, the tumor/control organ (brain) homing ratio for fd-tet phage was 6.5, compared with tumor/control organ homing ratios of 25 for the RGD-4C phage and 26 for the chimera phage. These data show a 4-fold accumulation of targeted phage in tumors. This result was further corroborated by immunohistochemistry (Figures 6B–6D), showing substantial RGD-4C and chimera phage localization in the tumor (Figures 6C and 6D) and only background staining from fd-tet phage-injected mice (Figure 6B). Control organs (such as brain and liver) from these mice were stained and showed similar staining patterns for all three phage (data not shown).

Qdot signals are particularly challenging to detect

in vivo; most of the applications described thus far focus on cell imaging in vitro. However, we could easily identify Qdots targeted to α_v integrins in the tissues examined. Strong fluorescence was detected in the tumors of mice that received the chimera phage-Qdot complex intravenously (Figures 6E–6G) but not in the tumors of mice that received RGD-4C phage-Qdot or fd-tet phage-Qdot (Figures 6H–6J). Together, these data show that the chimera phage-Qdot complex can be targeted to tumors in vivo.

Discussion

Chemical reactions to produce active targeted bioconjugates are widely used in a variety of biotechnology applications. Such conjugates consist of an effector bioactive agent and a targeting-carrier moiety that confers specificity of action, increases drug load, or avoids common clearance mechanisms [1]. However, several technical problems can hinder the production of effective targeted agents. Mild conditions are required to maintain the activity of the bioconjugate components (more when activation of the conjugate counterparts is needed), and yield is generally low. Changes in hydrophobicity and molecular weight of the resulting conjugate can also result in loss of solubility. These obstacles may either prevent the production or alter the pharmacologic characteristics of desired conjugates.

Phage display has been used for antigen-antibody epitope mapping, identification of protein binding sites in receptor-ligand interactions, enzyme functional domain inhibition, cell targeting, and even for direct selection in patients [2–7, 16, 23]. Importantly, methodology for phage ELISA using the appealing concept of bifunctional phage has long been developed [10, 11]. However, several considerations to bifunctional phage systems merit further comment. Among them are affinity of the complexes, reduction on the effective density of ligands of interest, and in vivo stability. As far as affinity of the complexes, we believe the data presented here provide sound evidence of the binding capacity of the phage to various surfaces. In the settings tested (coated plastic, magnetic beads, BIAcore chips, and Qdots), phage bound in a stable, though not always quantifiable, manner. Follow-up comparisons of the chimeric phage construct to chemically biotinylated RGD-4C phage, although technically challenging, might yield additional data. Despite the considerable reduction on the effective density of ligands when phage are used—as phage occupies most of the surface of interest when the particle is immobilized—this approach can still be possible, as evident from previous reports [10, 11] and from the work presented here. Still, this important issue must be carefully considered when designing experiments and may limit certain applications. Finally, as to the in vivo stability, indeed, no one has yet conducted a methodical study of the integrity of the complex. However, we show that in some cases the stability of the phage-streptavidin conjugate complex is high enough to allow delivery of large complexes to their target site. The dotted pattern of fluorescence in the tumor for the chimera-Qdot indicates stability, at least for a short circulation timeframe. Although the nature of the observed aggregates has not yet been explored in detail, this distribution pattern suggests that other complexes based on streptavidin conjugates (e.g., macromolecule-based drug carriers, liposomes, and polymeric drug delivery systems) may be targeted and exert their effect in the tumor tissue. Moreover, while phage particles accumulate in organs that are part of the reticulo-endothelial system, such as liver and spleen, receptor-mediated internalization does not appear to take place in such sites. This is an aspect that favors targeted intracellular delivery in this system.

Phage display technology is widely available and can be easily adapted to any biological system studied. After identification of a peptide motif or an Ab-phage clone that interacts specifically with a target molecule, various applications can be immediately developed to study and target the new molecule. Although other chemical and biological targeting strategies may be more suitable in some settings [24], this system may enhance the capabilities of monitoring binding and trafficking in cellular assays. Such a simple means of detecting and following phage clones after binding to cellular receptors of interest would likely enhance our understanding of many newly discovered molecular targets.

In summary, the work presented here demonstrates that a bifunctional phage can capture or target probes to cells expressing receptors of interest while avoiding complex chemical conjugations. Targeting beads or Qdots and phage immobilization onto different surfaces—such as microarray chips, colloidal particles, or various solid phases—may yield new tools for the discovery and characterization of molecular targets. Collectively, the experiments described extend the concept of bifunctional phage display into several potentially useful research and preclinical applications.

Significance

Targeted delivery of agents to tumors may form the basis of a new pharmacology that exploits biochemical differences on the surface of cancer cells and of those cells forming tumor-associated blood vessels. However, efficient application of this concept has been hindered by the complex chemistry and difficulty in the reliable production of bispecific conjugates. The proof-of-principle presented here shows that it is possible to develop biologically active particles that target cell surface receptors. This practical and convenient modular system may allow easy selection and characterization of functional protein-protein interactions and their integration with other technologies toward translational applications.

Experimental Procedures

Generation of a Bifunctional Phage Vector

To create a chimera phage, unique restriction sites present at similar locations in the plasmid DNA of two existing phage were chosen. In both, a BamHI site is located about 670 bp downstream from the pIII gene initiation codon. An XbaI site is located 4 bp downstream from the initiation codon of the tetracycline (Tet) repressor protein gene. DNA extracted from a fUSE5 vector (clone RGD-4C) [12] and an f88-Cys5 vector (clone R5C2, NCBI accession #AF246454) [25] was used to transform MC1061 *Escherichia coli*. Single colonies selected on Luria-Bertami (LB) agar plates containing streptomycin and tetracycline were cultured overnight, and plasmid DNA was extracted by using a plasmid purification kit (Qiagen, Valencia, CA).

One microgram of DNA from each clone was digested with XbaI and BamHI restriction endonucleases (Roche, Mannheim, Germany). The digested DNA was resolved on a 0.8% agarose gel, and the desired DNA fragments (i.e., a 3925 bp fragment from RGD-4C plasmid and a 5402 bp fragment from R5C2 plasmid) were extracted and purified using a gel purification kit (Qbiogene, Vista, CA). DNA fragments were ligated overnight at 16°C with T4 DNA ligase (Life Technologies, Grand Island, NY). The ligation product was electroporated into MC1061 *E. coli* and plated on LB-agar plates containing tetracycline and streptomycin. Restriction digests of plasmid DNA from multiple colonies were analyzed on E-Gels (Invitrogen, Carlsbad, CA). Sequences were confirmed by PCR with specific primers.

Chimera Phage Binding to Streptavidin

Phage from double-insert-positive clones were purified using the polyethylene glycol-NaCl method [2]. To test the binding of phage to streptavidin, we used streptavidin high binding capacity plates (Reacti-Bind, Pierce, Rockford, IL). One billion phage transducing units (TU) in PBS containing 2% bovine serum albumin (BSA) were incubated in triplicate wells for 2 hr at room temperature (RT) and washed with PBS containing 0.01% Tween-20 (PBST). For inhibition experiments, biotin (Sigma Chemical Co., St. Louis, MO) was mixed with the phage before incubation on the plate. Phage binding was measured by ELISA by using a horseradish peroxidase (HRP)/anti-M13 monoclonal Ab (mAb) conjugate (Amersham Biosciences, Piscataway, NJ) and developed with 3, 3′, 5, 5′-tetramethylbenzidine (Calbiochem, La Jolla, CA). Absorbance at 450 nm was determined in a plate reader (Bio-Tek Instruments Inc., Winooski, VT). For the streptavidin hybridization, 5×10^9 phage TU were denatured and resolved on a Novex 16% polyacrylamide gel electrophoresis (PAGE)-tricine (Invitrogen) and transferred to Trans-Blot nitrocellulose membrane (Bio-Rad, Hercules, CA). The membrane was blocked with 3% BSA in Tris-buffered saline containing 0.01% Tween-20 and incubated with HRP-conjugated streptavidin (Amersham Biosciences UK, Buckinghamshire, England) overnight at 4°C. Blots were washed three times with PBST and developed with the enhanced chemiluminescence (ECL) plus reagent (Amersham Biosciences UK) for 3 min. Membrane was exposed to HyperFilm ECL film (Amersham Biosciences UK) for detection.

$pIII_{D1}$ Preparation and Purification

The $pIII_{D1}$ coding regions from insertless fd-tet phage or phage displaying the RGD-4C peptide were amplified directly from phage DNA through PCR by using the primer sets: 5′-CCTTTCTATTCTCA TATGGCCGACGGGGC-3′/5′-CTCAGAACCGCCACCCTCGAGGCC ACC-3′ (for RGD-4C), or 5′-CGCGAATTCTTATTATTCGCAATTCCT TTAGTTG-3′/5′-CTCAGAACCGCCACCCTCGAGGCCACC-3′ (for fd-tet). PCR products were digested with NdeI and XhoI (RGD-4C phage) or EcoRI and XhoI (fd-tet phage) and subcloned into the pET21a vector (Novagen, Madison, WI). The constructs were sequenced, and the recombinant proteins were expressed in *E. coli* BL21 DE3 (Novagen). Induced recombinant proteins were purified from bacterial extracts under native conditions using a Ni^{2+}NTA-agarose column (Qiagen). Protein purity greater than 95% was determined on sodium dodecyl sulfate (SDS)-PAGE. For cell adhesion assays, 48-well plates were coated with $pIII_{D1}$-RGD-4C, $pIII_{D1}$-fd or vitronectin (20 μg/ml each) and blocked in PBS containing 3% BSA. Human Kaposi's sarcoma-derived cells (KS1767) were detached with 2.5 mM PBS-EDTA, resuspended in modified Eagle's medium (MEM), and added to the wells (10^5 cells/well). After 1 hr, unattached cells were removed by gentle washing, and attached cells were fixed in 4% PBS-buffered paraformaldehyde (PFA). Images were acquired on a phase-contrast microscope.

Testing Phage Binding to Cell Surface Integrins

An established aqueous-organic phase separation method was used to assess phage binding [16]. Briefly, 10^5 human Kaposi's sarcoma-derived cells KS1767 were harvested in 2.5 mM PBS-EDTA and incubated with 10^9 phage TU in modified Eagle's medium (MEM) containing 2% BSA, with or without 400 μg of $pIII_{D1}$ fusion proteins, for 3 hr at 4°C. Cells were loaded on 200 μl of 9:1 (v/v) dibutyl phthalate:cyclohexane (Aldrich Chemical Co., Milwaukee, WI) and centrifuged at 4°C for 10 min. Pellets were infected with log-phase K91Kan *E. Coli* for 1 hr, plated, incubated, and quantified. For immunocytochemical analysis of phage binding, 10^5 KS1767 cells were seeded in a 48-well tissue culture plate and allowed to attach overnight at 37°C. Next, 5×10^9 phage TU were added to the cells, with or without 400 μg of $pIII_{D1}$ fusion proteins, and incubated for 2 hr at RT. Bound phage were detected with anti-fd bacteriophage Ab (Sigma) and a FITC-conjugated secondary Ab. Cells were then fixed with PFA and visualized by fluorescence microscopy.

Binding of the Chimera Phage via Both Peptide Display Systems

In cell overlay assays, 5×10^9 TU of phage were incubated on streptavidin ReactiBind plates (Pierce) for 2 hr at RT and washed with PBST. KS1767 cells were then added in triplicate (10^4 cells/well) and incubated for 2 hr, and wells were washed and fixed with PFA. Cells in each group were counted under a phase-contrast microscope. For cell capture with magnetic beads, 10^9 phage TU were combined with 10 μl (~0.1 mg) of Dynabeads M-280 streptavidin-coated beads (Dynal, Oslo, Norway) in binding buffer (5 mM Tris-HCl [pH 7.5], 0.5 mM EDTA, 1 M NaCl) for 90 min at RT and washed three times with binding buffer in an MPC-S magnetic apparatus (Dynal). Beads were resuspended in 200 μl of PBS, mixed with 5×10^4 cells in PBS containing 2% BSA, agitated for 90 min, washed twice, and resuspended in PBS containing 2% BSA. Cells were plated in a 48-well tissue culture plate, incubated overnight at 37°C, fixed in PFA, and examined under a phase-contrast microscope. For quantification, 0.5% crystal violet dye in 20% methanol was added to each well. Wells were washed with water, bound dye was dissolved in 50 μl of 1:1 (v/v) 0.1 M sodium citrate (pH 6.0):methanol, and absorbance at 550 nm was determined.

Cell-Surface Detection of Bound Phage with Fluorescent Beads

KS1767 cells (10^5 per well in a 48-well plate) were incubated in duplicates with 10^{10} TU of chimera, RGD-4C, R5C2, or fd-tet phage in MEM containing 2% BSA for 2 hr at RT. After washing, 10^{11} streptavidin-coated or uncoated red-orange fluorescent microspheres (Molecular Probes, Eugene, OR) were added in 200 μl of BlockAid solution (Molecular Probes) for 2 hr. Cells were washed, fixed in PFA, and examined under a fluorescence microscope. To validate reactivity of streptavidin on fluorescent beads toward biotin, cells were incubated with anti-M13 pVIII mAb (Amersham Bioscience) and a biotinylated secondary Ab (Sigma). Cells were then treated with streptavidin-coated beads and evaluated by fluorescence microscopy.

Surface Plasmon Resonance

Streptavidin-coated chips (BIAcore AB, Uppsala, Sweden) were immobilized with purified 10^{11} TU/ml of chimera or R5C2 phage in two separate channels by injecting the phage suspension in two consecutive cycles of 20 μl/min for 6 min in a biosensor (BIAcore AB). Similar signals were achieved. Single-cell suspensions of freshly harvested KS1767 cells in PBS were injected over all the channels at 10^5 cells/ml for 10 min and sensograms recorded. The on-rates were calculated from the slopes of the log phase in the sensograms. All stages were conducted at 25°C. Data acquired were processed through software provided by the manufacturer.

Cell Targeting of Qdot-Labeled Chimera Phage

Qdot 605 streptavidin (Quantum Dot, Hayward, CA) was mixed with chimera, RGD-4C, or R5C2 phage (at 5×10^9 TU each) in duplicates and incubated under rotation at RT for 45 min. Each admixture was added to 10^5 adherent KS1767 cells in a Lab-Tek II chamber slide (Nalge Nunc, Naperville, IL) in MEM containing 2% BSA and incubated for 2 hr at RT or 24 hr at 37°C for the internalization assay. Cells incubated for 2 hr were washed, incubated with anti-M13 mAb and anti-mouse IgG FITC conjugate (Sigma), and fixed with PFA. For the internalization study, cells were washed with 50 mM glycine/500 mM NaCl buffer, fixed with PFA, permeabilized with 0.2% Triton X-100 solution, blocked with 1% BSA in PBS solution, then incubated with anti-M13 mAb and the secondary FITC conjugate, and fixed again in PFA. Slides were mounted with Mowiol 4-88 (Poly-

sciences, Eppelheim, Germany), visualized under an epi-fluorescent microscope, and microphotographed by using a UV-blue filter.

Targeting Phage-Qdot Complexes to Tumors in Mice

Eight-week-old Balb/C mice were inoculated subcutaneously with 10^5 EF43.*fgf-4* cells [21] in the right flank, and tumors were allowed to grow for 2 weeks to an approximate diameter of 8 mm. Ten billion TU of chimera, RGD-4C, or fd-tet phage were allowed to react for 1 hr with 40 nM of Qdot 605 streptavidin at RT. Mice were then injected via the lateral tail vein with 10 μl of the mixture and perfused through the heart after 5–8 min circulation with 5 ml of MEM containing proteinase inhibitor cocktail (Sigma)-0.1% BSA. Tumor, brain, liver, and kidneys from each mouse were surgically removed and divided for phage recovery or immunohistochemistry. For phage recovery, organs were weighed, homogenized, and washed; phage rescue was performed by incubating the homogenates with 0.5 ml of K91kan *E. coli* for 1 hr at RT, diluting the mixtures 1:10 in LB medium, incubating for another 30 min at 37°C, and then plating in aliquots on agar plates containing Tet and kanamycine. Sections from formalin-fixed paraffin-embedded tissues were stained as described [2]. Briefly, samples were deparaffinized, blocked for peroxidase activity, antigen-retrieved by heat in EDTA solution (Zymed, South San Francisco, CA), protein blocked (Dako, Carpinteria, CA), and incubated with anti-fd bacteriophage or control Ab (both from Sigma). The EnVision+ system (Dako) and DPX Mountant (Fluka, Milwaukee, WI) were used for detection and mounting, respectively. For fluorescence localization, slides were deparaffinized, mounted, and then observed under an epi-fluorescent microscope using a UV-blue excitation filter.

Acknowledgments

We thank Dr. David Needleman for technical assistance and Drs. David LaVan and George P. Smith for advice and comments on an earlier version of the manuscript. This work was supported by National Institutes of Health grants CA90270 (to R.P. and W.A.), CA82976, CA78512, and CA88106 (to R.P.), and CA103042 and CA90810 (to W.A.), National Cancer Institute R01-DK67683 (to W.A.), Department of Defense DAMD17-03-1-0384 (to R.P.), and by awards from the Gilson-Longenbaugh Foundation, the V Foundation, and AngelWorks (all to R.P. and W.A.). A.J.Z. is the recipient of a fellowship from the Instituto de Salud Carlos III, Spain (BEFI 01/9526).

Received: March 24, 2004
Revised: May 12, 2004
Accepted: May 18, 2004
Published: August 20, 2004

References

1. Hermanson, G.T. (1996). Homobifunctional cross-linkers. In Bioconjugate Techniques, G.T. Hermanson, ed. (San Diego: Academic Press), pp. 187–227.
2. Webster, R. (2001). Filamentous phage biology. In Phage Display: A Laboratory Manual, C.F. Barbas, III, D.R. Burton, J.K. Scott, and G.J. Silverman, eds. (Cold Spring Harbor, NY: Cold Spring Harbor Laboratory Press), pp. 1.1–1.37.
3. Hoogenboom, H.R. (2002). Overview of antibody phage-display technology and its applications. Methods Mol. Biol. *178*, 1–37.
4. Smith, G.P. (1985). Filamentous fusion phage: novel expression vectors that display cloned antigens on the virion surface. Science *228*, 1315–1317.
5. Scott, J.K., and Smith, G.P. (1990). Searching for peptide ligands with an epitope library. Science *249*, 386–390.
6. McCafferty, J., Griffiths, A.D., Winter, G., and Chiswell, D.J. (1990). Phage antibodies: filamentous phage displaying antibody variable domains. Nature *348*, 552–554.
7. Smith, G.P., and Scott, J.K. (1993). Libraries of peptides and proteins displayed on filamentous phage. Methods Enzymol. *217*, 228–257.
8. Zacher, A.N., III, Stock, C.A., Golden, J.W., II, and Smith, G.P. (1980). A new filamentous phage cloning vector: fd-tet. Gene *9*, 127–140.
9. Gao, C., Mao, S., Kaufmann, G., Wirsching, P., Lerner, R.A., and Janda, K.D. (2002). A method for the generation of combinatorial antibody libraries using pIX phage display. Proc. Natl. Acad. Sci. USA *99*, 12612–12616.
10. Light, J., and Lerner, R.A. (1992). Phophabs: antibody-phage-alkaline phosphatase conjugates for one step ELISA's without immunization. Bioorg. Med. Chem. Lett. *2*, 1073–1078.
11. Bonnycastle, L.L., Brown, K.L., Tang, J., and Scott, J.K. (1997). Assaying phage-borne peptides by phage capture on fibrinogen or streptavidin. Biol. Chem. *378*, 509–515.
12. Ruoslahti, E. (1996). RGD and other recognition sequences for integrins. Annu. Rev. Cell Dev. Biol. *12*, 697–715.
13. Pasqualini, R., Koivunen, E., and Ruoslahti, E. (1997). Alpha v integrins as receptors for tumor targeting by circulating ligands. Nat. Biotechnol. *15*, 542–546.
14. Katz, B.A., and Cass, R.T. (1997). In crystals of complexes of streptavidin with peptide ligands containing the HPQ sequence the pKa of the peptide histidine is less than 3.0. J. Biol. Chem. *272*, 13220–13228.
15. Wilchek, M., and Bayer, E.A. (1990). Introduction to avidin-biotin technology. Methods Enzymol. *184*, 5–13.
16. Giordano, R.J., Cardó-Vila, M., Lahdenranta, J., Pasqualini, R., and Arap, W. (2001). Biopanning and rapid analysis of selective interactive ligands. Nat. Med. *7*, 1249–1253.
17. Bhalgat, M.K., Haugland, R.P., Pollack, J.S., and Swan, S. (1998). Green- and red-fluorescent nanospheres for the detection of cell surface receptors by flow cytometry. J. Immunol. Methods *219*, 57–68.
18. McDonnell, J.M. (2001). Surface plasmon resonance: towards an understanding of the mechanisms of biological molecular recognition. Curr. Opin. Chem. Biol. *5*, 572–577.
19. Bruchez, M.P., Morrone, M., Gin, P., Weiss, S., and Alivisatos, P.A. (1998). Semiconductor nanocrystals as fluorescent biological labels. Science *281*, 2013–2016.
20. Rosenthal, S.J., Tomlinson, I., Adkins, E.M., Schroeter, S., Adams, S., Swafford, L., McBride, J., Wang, Y., DeFelice, L.J., and Blakely, R.D. (2002). Targeting cell surface receptors with ligand-conjugated nanocrystals. J. Am. Chem. Soc. *124*, 4586–4594.
21. Hajitou, A., Baramova, E.N., Bajou, K., Noe, V., Bruyneel, E., Mareel, M., Collette, J., Foidart, J.M., and Calberg-Bacq, C.M. (1998). FGF-3 and FGF-4 elicit distinct oncogenic properties in mouse mammary myoepithelial cells. Oncogene *17*, 2059–2071.
22. Pasqualini, R., and Arap, W. (2002). Vascular targeting. In Encyclopedia of Cancer, J.R. Bertino, ed. (San Diego: Academic Press/Elsevier Science), pp. 501–507.
23. Arap, W., Kolonin, M.G., Trepel, M., Lahdenranta, J., Cardó-Vila, M., Giordano, R.J., Mintz, P.J., Ardelt, P.U., Yao, V.J., Vidal, C.I., et al. (2002). Steps toward mapping the human vasculature by phage display. Nat. Med. *8*, 121–127.
24. Hood, J.D., Bednarki, M., Frausto, R., Guccione, S., Reisfeld, R.A., Xiang, R., and Cheresh, D.A. (2002). Tumor regression by targeted gene delivery to the neovasculature. Science *296*, 2404–2407.
25. Weber, P.C., Pantoliano, M.W., and Thompson, L.D. (1992). Crystal structure and ligand-binding studies of a screened peptide complexed with streptavidin. Biochemistry *31*, 9350–9354.